IEEE Access
Multidisciplinary ⋮ Rapid Review ⋮ Open Access Journal

Received August 19, 2020, accepted August 31, 2020, date of publication September 15, 2020, date of current version September 25, 2020.

Digital Object Identifier 10.1109/ACCESS.2020.3024100

Direct Cell Counting Using Macro-Scale Smartphone Images of Cell Aggregates

CHIKAHIRO IMASHIRO[1,2], YUTA TOKUOKA[3], KAITO KIKUHARA[4,5], TAKAHIRO G. YAMADA[3,6], KENJIRO TAKEMURA[1], (Member, IEEE), AND AKIRA FUNAHASHI[6]

[1]Department of Mechanical Engineering, Keio University, Yokohama 223-8522, Japan
[2]Institute of Advanced Biomedical Engineering and Science, Tokyo Women's Medical University, Tokyo 162-8666, Japan
[3]School of Fundamental Science and Technology, Graduate School of Science and Technology, Keio University, Yokohama 223-8522, Japan
[4]Graduate School of Media and Governance, Keio University, Fujisawa 252-0882, Japan
[5]School of Science for Open and Environmental Systems, Graduate School of Science and Technology, Keio University, Yokohama 223-8522, Japan
[6]Department of Bioscience and Bioinformatics, Keio University, Yokohama 223-8522, Japan

Corresponding author: Akira Funahashi (funa@bio.keio.ac.jp)

This work was supported in part by the JSPS KAKENHI under Grant JP16H04259, Grant 16H04731, Grant JP17H07081, Grant 18J12482, and Grant 19J13189; and in part by the MEXT Grant-in-Aid for the Program for Leading Graduate Schools.

ABSTRACT The field of bioengineering depends on technologies for stable cell culture. Conventionally, every process involved in cell culture has been performed manually, so the culture efficiency and stability can vary between trials or depending on the technician. Among these processes, cell counting is particularly important because cell density affects cell function. Conventional cell counting techniques for cell number estimation are inefficient and unstable because they involve the manual work of collecting a sample of the cell suspension. Thus, a cell counting method that is not susceptible to human error is needed. In this study, we present a novel cell counting method based on smartphone imaging and convolutional neural network-based image processing. Cells are aggregated by centrifuging in a tube and then imaged using a smartphone. The image is transferred to a server, and the cell number is predicted using convolutional neural networks on the server. All processes are performed by a custom-developed smartphone-compatible web app. Compared with the conventional method using a hemocytometer, our method yields more stable cell counting. Furthermore, the time and labor required for cell counting are significantly reduced. Our new method could potentially replace conventional cell counting techniques and thus enhance the stability and efficiency of bioengineering studies that require cell culture.

INDEX TERMS Cell counting, cell culture process, regression analysis, supervised learning, computational biology, machine learning, convolutional neural network.

I. INTRODUCTION

Studies in bioengineering, including tissue engineering, regenerative medicine, organ-on-a-chip, and biomedicine studies [1], [2], require stable and effective cell culture methods. Cell culture processes involve seeding, detaching, and reseeding cells. The density of cultured cells is known to affect their function and proliferation rate, so the number of seeded cells must be measured and adjusted before seeding [3]–[5]. Conventionally, every process involved in cell culture is performed manually. However, manual steps present a risk of contamination and result in variable culture efficiency and stability between trials and depending on the technician [6]. In the interest of standardizing these processes, several techniques have been developed, such as cell patterning, detaching, collecting, and harvesting [7]–[12]. Cell counting technologies, which are key to realizing stable and effective cell culture, have been developed, but they require dedicated devices or labor-intensive processes [13], [14].

The most widely used conventional cell counting method consists of several steps, as shown in Fig. 1a. First, a sample of the cell suspension is collected from the suspension containing all cells. Second, the sample is loaded into a hemocytometer mounted on a microscope. Finally, the cell density of the sample is measured by a technician and used to calculate the number of cells in the suspension, assuming that the cell density of the sample is equal to that of the suspension. This manual process is tedious and time consuming, increasing the burden on technicians. Because the counted

The associate editor coordinating the review of this manuscript and approving it for publication was Rajeswari Sundararajan.

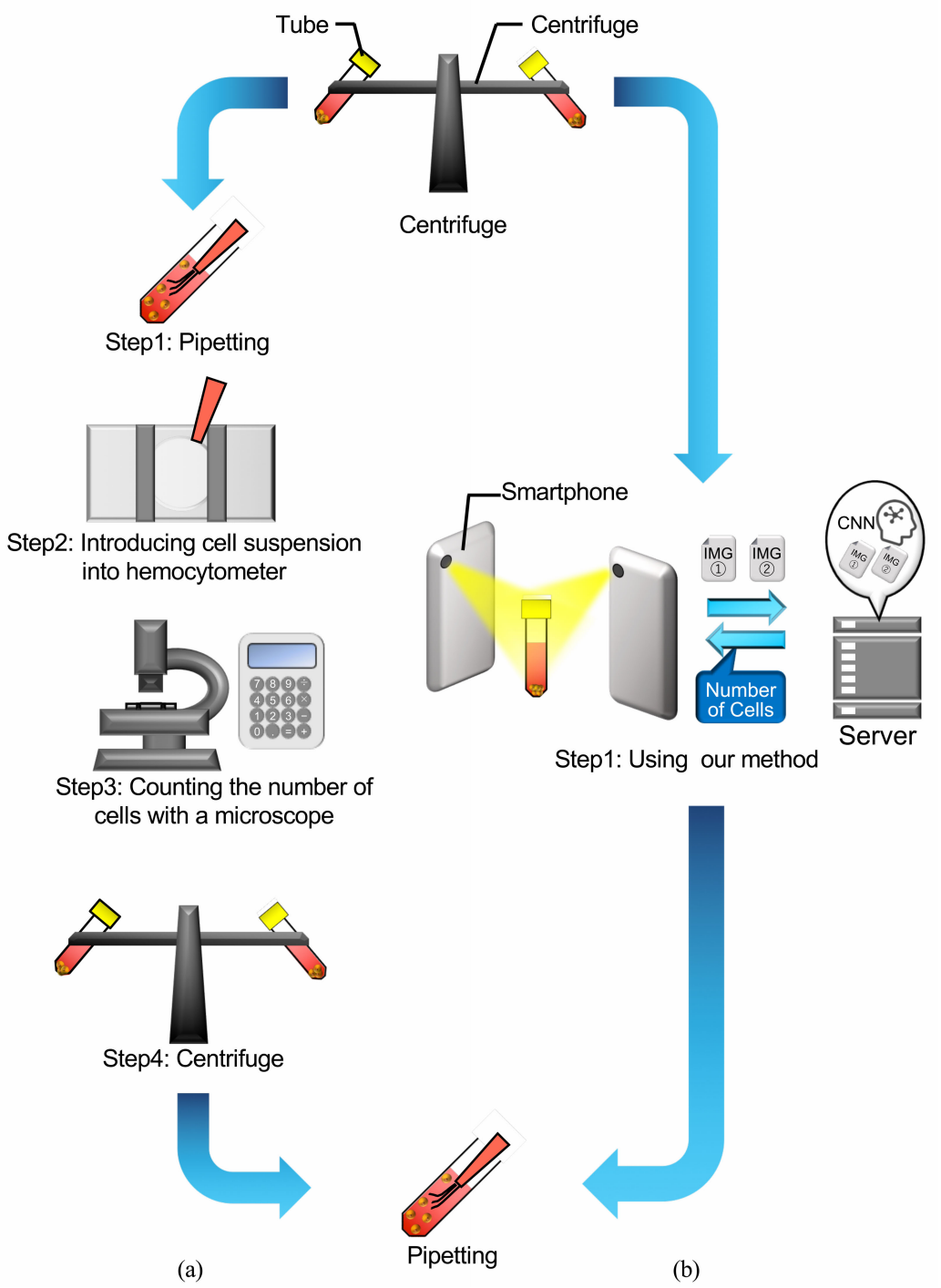

FIGURE 1. Comparison of cell counting by (a) the conventional method and (b) the proposed method. While the conventional method comprises four steps, the developed app requires only a single step.

cells cannot be reused, this process wastes cells that may be difficult to obtain. Moreover, the estimation of cell density in the suspension is susceptible to human error (for example, when counting cells on the microscope) and depends on the skill of the technician; therefore, the results tend to vary from technician to technician. The added steps also increase the risk of contamination.

Several cell counting methods based on cutting-edge technologies, such as image analysis, electronics, and optics, have been proposed [15]–[16]. Most of these methods are performed with a sample of cells from the cell suspension. Of these methods, image analysis-based techniques have been most commonly implemented in practical applications. An automated cell counter designed to decrease the

technician burden and risk of miscounting has been developed and commercialized [17]. The cell suspension is introduced into a dedicated chamber, and the device automatically measures the cell density in the sample. While this tool does reduce the time and labor required for cell counting, the measurement may still be susceptible to error because it still requires manual sampling of the cell suspension. Another method based on image analysis is based on counting cells from microscopic images of cells adhered to a culture surface [18]. Manual sampling is not required with this approach. However, because the density of cultured cells is not homogeneous, the accuracy of the predicted cell number is influenced by the cell seeding techniques used by technicians [19]. In contrast, optics-based methods can be used to measure the number of cells in the entire cell suspension, but they require dedicated and costly devices and labor-intensive procedures and can be used only for cell suspensions in which the approximate cell number is known [16]. Thus, a novel cell counting method that is more practical and robust against error is still required.

As mentioned above, almost all previously developed methods for cell counting require sampling of the cell suspension, which introduces many issues. Although several attempts have been made to replace the entire manual cell culture process with a fully automated system, no method of automated cell counting has been applied in practice [20]. To address the limitations of conventional approaches, the cell number should be measured directly in a suspension to prevent technician error and variation due to technician skill and thus obtain consistent results. Furthermore, decreasing the number of steps involved in the process is helpful for reducing the time cost and risk of contamination.

Hence, we proposed a technique involving the use of macro-scale images showing all cells in a suspension. Because single cells cannot be observed or counted in a macro-scale image as a result of their small size, we focused on the only moment at which cells can be observed even with the naked eye: immediately after centrifugation, when the cells are aggregated at the bottom of the tube. Skillful and experienced technicians are sometimes able to predict the number of aggregated cells after centrifugation, which demonstrates the potential for estimating the cell number at this stage. Deep learning methods, especially convolutional neural networks (CNNs), have been successful in various computer vision tasks such as classification, segmentation, and regression [21]–[25]. Thus, we used deep learning with CNNs to analyze images and predict the cell number from macro-scale images of aggregated cells.

On the basis of this approach, we developed a novel cell counting method in which an image of aggregated cells is captured by a smartphone and transferred to a server by a web application for smartphone. The CNN on the server then predicts the cell number (Fig. 1b). The use of ubiquitous smartphone technology offers fast computing, easy connectivity to servers, and a user-friendly interface [26]–[30]. The proposed method is simple and relatively quick, and provides superior accuracy and consistency for cell counting.

II. MATERIALS AND METHODS

A. OVERVIEW OF THE PROPOSED METHOD

Our method consists of three elements: image capture of aggregated cells, a web application for smartphones and a CNN. First, the aggregated cells in the tube are imaged from two directions using a smartphone. The second element, the smartphone-based web application, transfers these images from the smartphone to the server. Then, the CNN predicts the number of cells from the transferred images. The predicted cell number is transferred back to the smartphone *via* the web application. Therefore, in our method, the input is the centrifuge tube containing aggregated cells, and the output is the estimated cell number (Fig. 1b).

B. IMAGE CAPTURE

In general, datasets incorporating a large number of images captured with a range of imaging conditions need to be prepared to train the CNN to make robust inferences from images captured under various imaging conditions [29]. To minimize the number of training images required, we fixed the imaging conditions by using a jig to hold the centrifuge tube and smartphone, as shown in Fig. 2. With this jig, images can be taken from two directions with the exposure angle, lighting, and distance of the object from the camera kept constant.

Figure 2 shows the fabricated jig with a 15-mL centrifuge tube containing a cell suspension. The jig comprises two parts, each fabricated by a 3D printer (BCN3D SIGMA R19, BCN 3D Technologies, Barcelona, Spain): The upper part covers the side of the tube and fixes the tube position relative to the camera. The bottom part has a holder for the smartphone, a space holding a light-emitting diode (LED; LP-LED3SET), and a black wall. The black wall was integrated to shade the tube from direct illumination and thus prevent direct light from reflecting off of the surface of the tube, which would occlude the view of the cells. A 15-mL tube (TR2000, Nippon Genetics Co., Ltd., Tokyo, Japan) is set into the jig. The 3D model files of our developed jig are provided in the supplementary information. The smartphone holder fixes the smartphone upside-down at a constant distance of 80.6 mm from the tube. The LED illumination helps to maintain consistent illumination conditions.

To prepare cells for imaging, a cell suspension is centrifuged (H-19α, Kokusan, Saitama, Japan) in a 15-mL tube for 2 min at 370 $\times$ g. The cell density in the suspension is measured using an automatic cell counter (TC20TM Automated Cell Counter, Bio-Rad, CA, USA) three times as the reference standard.

C. DESIGN OF THE CNN

We implemented a CNN model that predicts the number of cells from images of aggregated cells taken from two

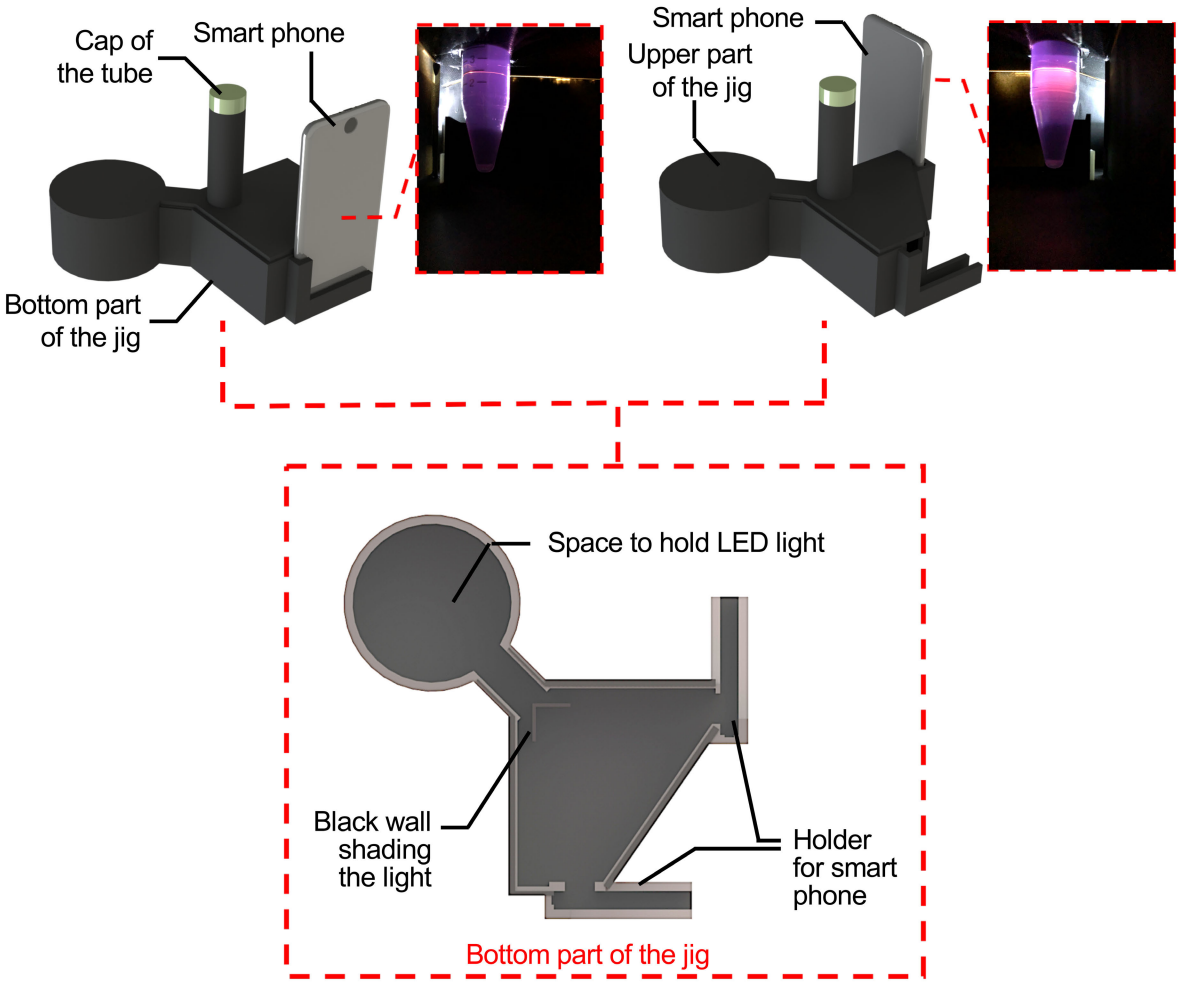

FIGURE 2. Structure fabricated to fix the conditions for capturing images.

directions (Fig. 3a). Our CNN model comprises consecutive convolutional layers, max pooling layers, and fully-connected layers. The last fully-connected layer consists of one neuron for the objective function (Fig. 3b). Every convolutional layer and all fully-connected layers except for the last are followed by rectified linear units [30]. We applied dropout (rate: 0.5) to the fully-connected layers [31]. Because the CNN model learns the task of regression, the mean-squared error was used for the objective function. The details of the hyperparameters of the CNN model are provided in Supplementary Table 1.

D. DESIGN OF THE CELL COUNTING APP

We designed a web application (herein referred to as cell counting app, CCA) to serve as an interface between the smartphone and the CNN model on a server. The CCA consists of three main components: a web-based user interface, a web server for providing an application programming interface (API) for cell counting, and a server for machine learning (Fig. 4). The user interface allows the user to upload two images and displays the counting results. The web server receives the images and carries out the analysis using the trained CNN model. This CNN model was trained by machine learning on the server and transferred to the web server in advance. The web-based CCA algorithm performs the following steps: (1) the images are received; (2) the CNN model carries out the image analysis; and (3) the user interface receives the result of the analysis (i.e., the number of cells).

The user interface and cell counting API were implemented in HTML, CSS, and Python 3.6. We developed separate Django applications to implement the API and user interface independently. The API for cell counting was implemented by using the Django web development framework because the API used to interface with the trained CNN model *via* Python is based on Django. The web server receives and saves the trained CNN model from the server for machine learning *via* the cell counting API. The user interface was designed with a single-page application concept using the Django template language with Bootstrap 4. The source code of the CCA is available from https://github.com/funalab/CellCountingApp.

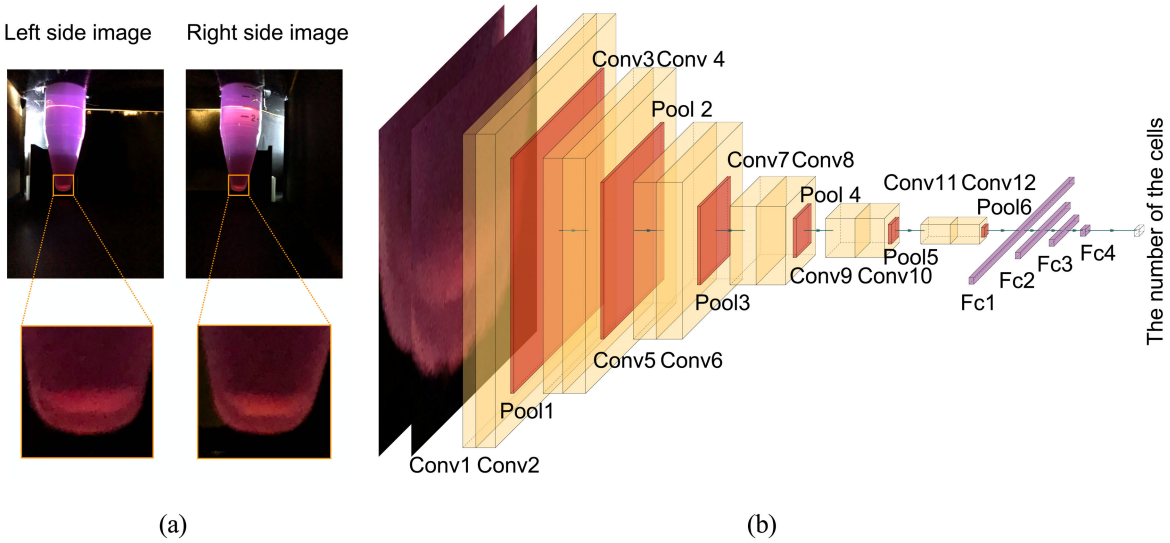

FIGURE 3. (a) Image pre-processing before input into the CNN model. (b) CNN architecture for predicting the number of cells. "Conv," "Pool," and "Fc" represent the convolution layer, pooling layer, and fully-connected layer, respectively.

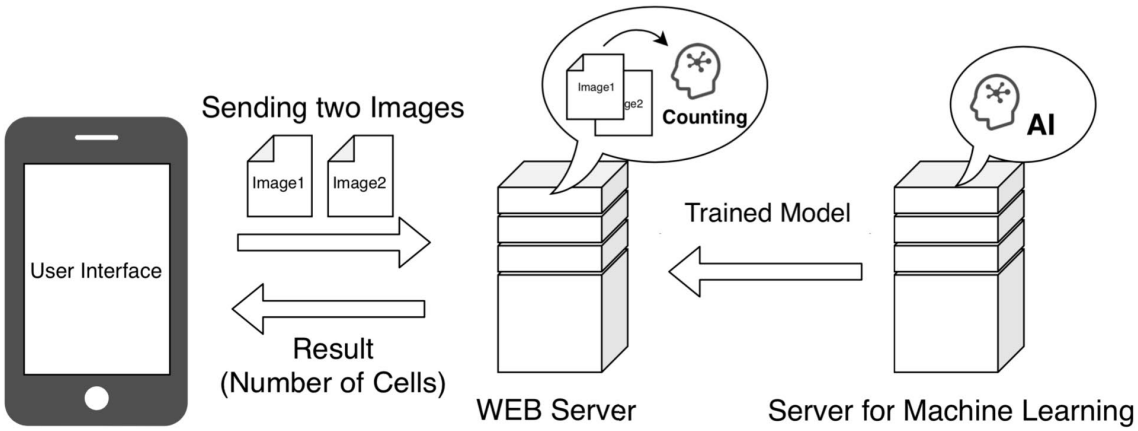

FIGURE 4. Schematic of the app designed for cell counting based on our CNN model.

E. PREPARATION OF THE TRAINING AND TEST DATASETS

We prepared a training dataset to train the CNN model. We captured images of cells centrifuged and aggregated at the bottom of the conical centrifuge tube using a smartphone (iPhone 8, Apple Inc., Cupertino, CA, USA) set into the jig; images were captured from two directions (Fig. 3a). The number of cells was varied from 1.0×10^6 cells to 1.0×10^7 cells in increments of 1.0×10^6 cells, and 50 image sets were acquired for each cell number. We defined the number of cells measured by the automatic cell counter as the true value. We divided these datasets into five subsets and performed cross-validation.

To evaluate the developed method, a test dataset was prepared in the same way as the training dataset. The numbers and the densities of cells in each sample were randomly determined. In addition, cell counting was also performed using a hemocytometer as a conventional cell counting method for comparison; the cell counting was repeated three times with the same sample. The datasets are available from https://github.com/funalab/CellCountingApp.

F. TRAINING PROCEDURE FOR THE CNN MODEL

We implemented and trained the CNN model using Chainer, an open-source software for deep learning [32]. We trained the CNN model with five-fold cross-validation. At each fold, we trained the CNN model for 100 epochs using Adam with mini-batches of five images. For each epoch, we evaluated the loss of the CNN model using validation data. The loss, L, was calculated based on the mean-squared error as follows:

$$L = \frac{1}{N} \sum_{i=1}^{N} (y_i - t_i)^2 , \tag{1}$$

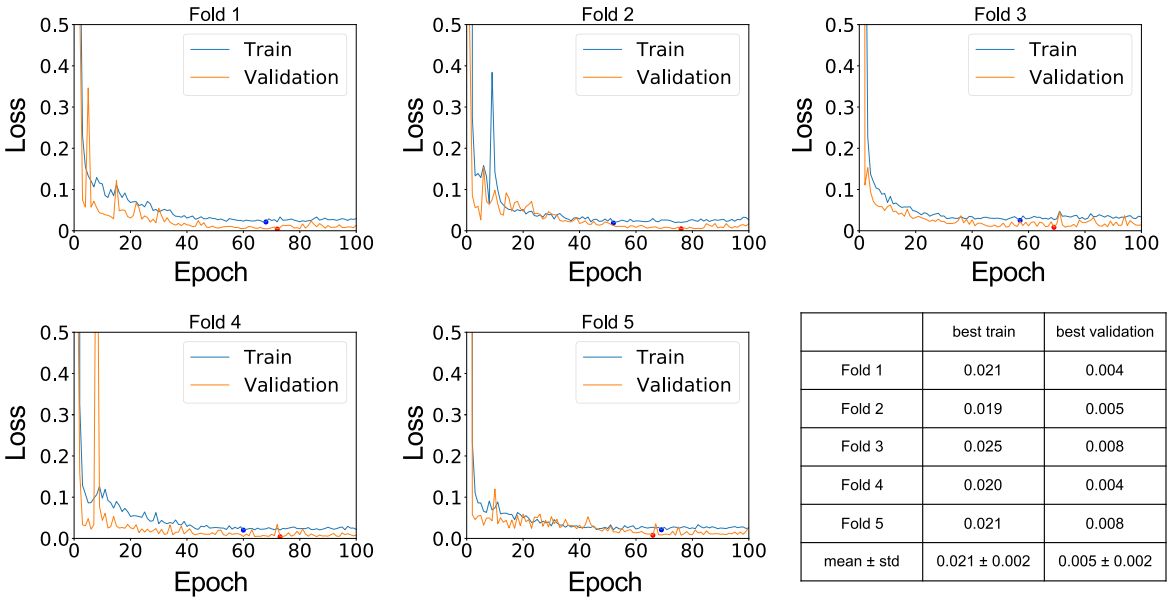

	best train	best validation
Fold 1	0.021	0.004
Fold 2	0.019	0.005
Fold 3	0.025	0.008
Fold 4	0.020	0.004
Fold 5	0.021	0.008
mean ± std	0.021 ± 0.002	0.005 ± 0.002

FIGURE 5. Results of CNN model training with five-fold cross validation. The vertical axis represents loss and the horizontal axis represents the epoch. The blue line represents the loss of the training dataset, while the orange line represents the loss of the validation dataset. The blue and red dot plots represent the epochs with the lowest losses in the training and validation datasets, respectively.

where N, y, and t represent the size of the mini-batches, the output, and the ground truth multiplied by 10^{-6}, respectively.

In the pre-processing step, a 320 × 320 pixel region of interest (i.e., the cell aggregate) was cropped from the original image (Fig. 3a). Then, data augmentation was performed by adding perturbation with a uniform distribution to the cropped image and randomly flipping the cropped image in the horizontal direction. These data augmentations were performed to prevent overfitting of the CNN model [31]. To ensure robustness against variations in illumination intensity, the pixel values of the cropped input image were normalized to the range of [0, 1] by subtracting the minimum pixel intensity and then dividing all pixel intensities by the difference between the maximum and minimum pixel intensities [33].

To compare the conventional cell counting method with our CNN model, we used the model with the least loss in cross-validation and applied it to the test data.

G. CELL PREPARATION

The mouse fibroblast cell line, L929 (RCB1451, Riken BioResource Center, Ibaraki, Japan), was used to demonstrate the proposed cell counting method. Cells were cultured in growth medium (modified Eagle's medium (MEM) "Nissui," Nissui Pharmaceutical Co., Ltd., Tokyo, Japan) supplemented with 5% fetal bovine serum (CELLect Gold, MP Biomedicals, Inc., CA, USA) in a 5% CO_2 humidified incubator at 37 °C. Cells were passaged by trypsinization in 0.050% trypsin-EDTA (25300, Life Technologies, CA, USA) with pipetting.

H. STATISTICAL ANALYSIS

We used a concordance correlation coefficient to evaluate the degree of agreement between the cell numbers determined by the proposed method and the true values [34]. The concordance correlation coefficient represents the variation between groups. We also used the F value to evaluate the variance in the cell numbers. The F value is the ratio of the variance in the group means to the mean of the variance within the group. The F test and unpaired Student's t-test were performed to compare the two groups. Values of $p < 0.05$ were considered statistically significant.

III. RESULTS

A. TRAINING AND VALIDATION OF THE CNN MODEL FOR PREDICTING THE NUMBER OF CELLS

We used the training dataset to train our CNN model by five-fold cross-validation and evaluated the training and validation loss for each epoch (Fig. 5). In every fold, the training and validation loss decreased with each epoch and converged. The mean of the lowest training loss across epochs was 0.021 ± 0.002, and the mean of the lowest validation loss across epochs was 0.006 ± 0.002. We defined the convergence model for each fold as the epoch with the lowest validation loss (Fig. 5, orange plot). The fold-1 model with the lowest loss was used for verification with the test dataset, as described in the next section.

B. EVALUATION OF OUR CNN MODEL

We compared our method with the conventional method in terms of accuracy and stability. Accuracy was defined relative

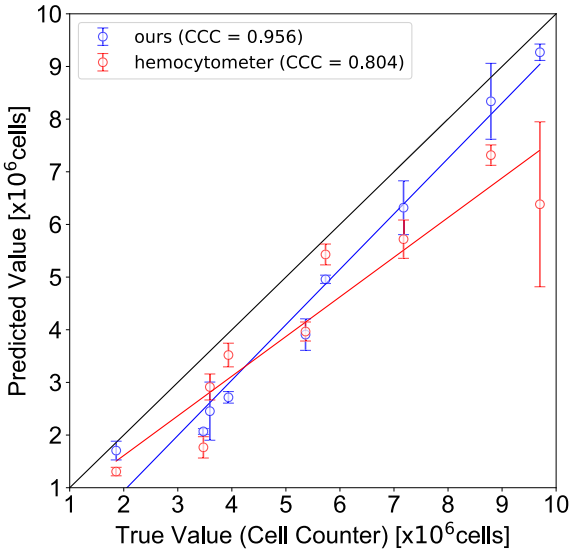

FIGURE 6. **Comparison of accuracy of the proposed cell counting method with that of the conventional hemocytometer-based method. The number of cells measured using Automated Cell Counter was regarded as the true value. The blue and red lines indicate linear fits to the results obtained using the proposed method and the hemocytometer, respectively. The black line represents the ground truth. CCC represents the concordance correlation coefficient. The predicted value is shown as mean ± SD.**

to the true value, while stability was defined as the consistency of the measurements. The concordance correlation coefficient and F value were used to evaluate each estimative metric.

First, the accuracy of each method was evaluated by comparing each measured value with the true value (Fig. 6); here, the number of cells measured by the automatic cell counter was considered as the true value. The concordance correlation coefficients of our method and the conventional method were 0.956 and 0.804, respectively. This finding indicates that the cell numbers estimated by our method were more accurate relative to the true value than those estimated using the conventional method, implying that the proposed method has higher accuracy than the conventional method.

The stability of each method was evaluated by plotting the cell numbers determined by our method or the conventional method against the true values and then determining the variance of the residuals of a linear fitted line. The variances for our method and the conventional method were 3.12×10^5 and 7.23×10^5 cells, respectively. The difference between these results was statistically significant (F value $= 2.32$, p-value of F test $= 0.03 < 0.05$). This result indicates that our method is more stable than the conventional method because it has a lower variance of residuals (i.e., prediction error).

C. DEMONSTRATION OF OUR METHOD

Next, we evaluated the entire proposed method from the viewpoints of the simplicity of the procedure and the time required to conduct the measurement.

To evaluate the simplicity of the proposed method, we compared the procedures of the conventional method and our method. As shown in Fig. 1(a), the conventional cell counting method using a hemocytometer involves four steps: After centrifugation, the supernatant is removed, and the cells are diluted in fresh medium to realize an appropriate cell density for counting (step 1). Then, a sample of the cell suspension is introduced into a hemocytometer, which must be washed daily (step 2). The hemocytometer is then mounted on a microscope, and the cell density is visually counted and used to calculate the total cell number (step 3). Finally, the sample is centrifuged once more (step 4) and resuspended in the volume of media needed to realize the desired cell density. In contrast, our method involves only a single step, namely using the CCA, as shown in Fig. 7; the remainder of the process is automated. One of the advantages of our method is that there is no need to maintain a homogeneous cell density. To use the CCA, the aggregated cells in the tube are imaged with a smartphone from the left side of the jig (sub-step 1-1) and again from the right side of the jig (sub-step 1-2). The captured images are then loaded into the appropriate location on the user interface of the CCA, and the 'Counting' button is pressed (sub-step 1-3). The estimated cell number is returned after tens of seconds (sub-step 1-4); the mean and standard deviation of the time from pressing the counting button to obtaining the result was 31.080 ± 3.806 *s* ($n = 10$). These findings demonstrate the simplicity and limited burden of the proposed method. Supplementary Movie 1 shows a comparison of the proposed and conventional cell counting methods.

We also measured the time required to carry out these two cell counting methods, as shown in Fig. 8. Our method was faster than the conventional method: while the conventional method (steps 1 through 4) required around 383.7 s, our method (a single step) required around 56.3 s, and this difference was statistically significant. This finding indicates that the proposed method realizes simple and quick cell counting.

IV. DISCUSSION

In this study, we demonstrate a novel automated smartphone-based cell counting method that is more convenient, accurate, and stable compared with the conventional hemocytometer-based cell counting method. The conventional technique is inconvenient because of the multiple steps and manual cell counting required. The proposed method can significantly reduce the time and involved procedures for counting cells. The use of smartphone technology with its seamless inputs and outputs of data enabled the rapid response of the proposed method. Furthermore, the required run-time of the proposed method is expected to be reduced in the near future as data transmission speeds increase. The steps required in the conventional method are complicated. A comparison of the proposed and conventional methods shows that our method could reduce the burden on technicians and the risk of contamination. Furthermore, the proposed method is promising not only from the viewpoint of functionality but also in terms of environmental protection; as shown in Supplementary Movie 1, the use of many consumables and washing of the

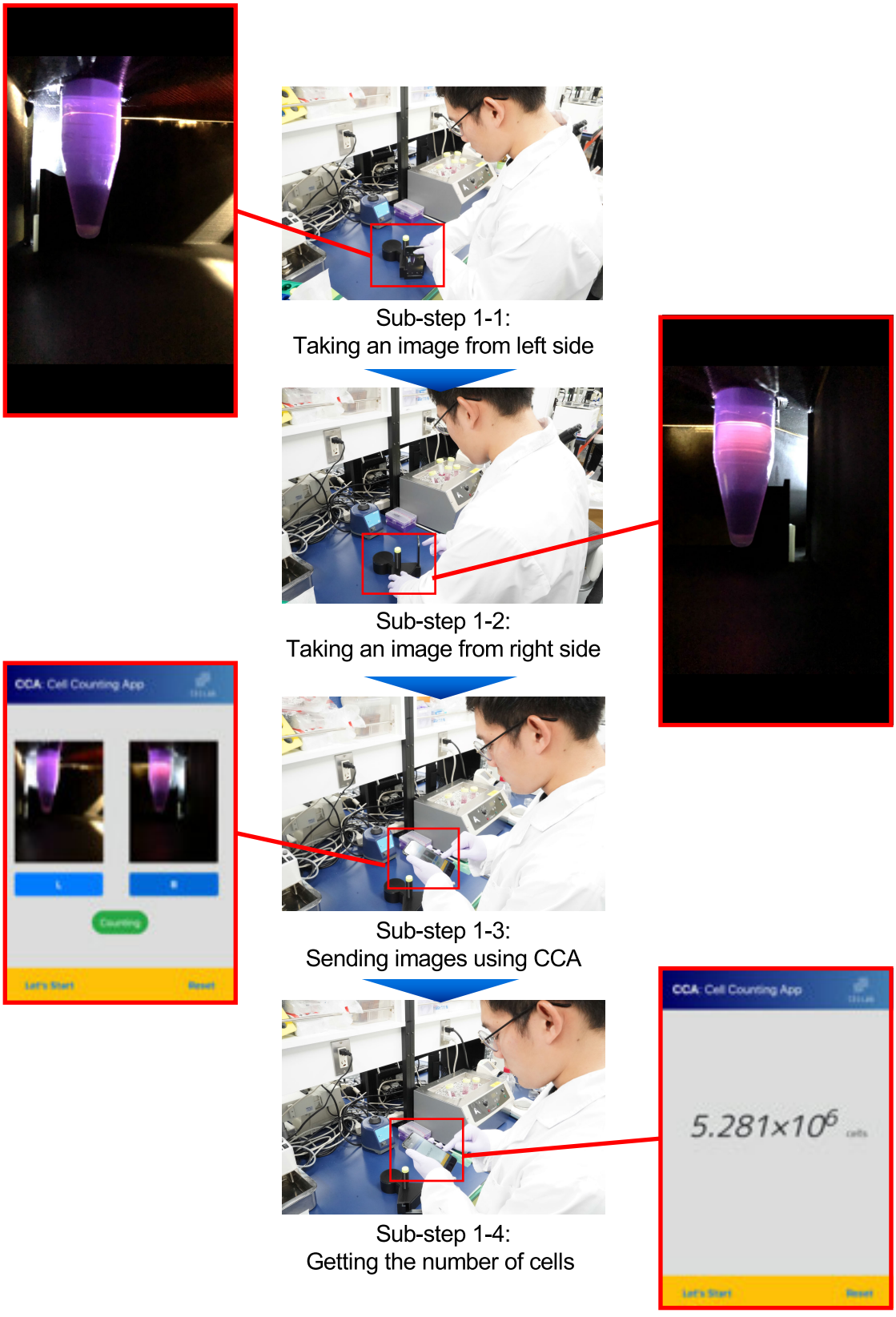

FIGURE 7. Demonstration of the use of CCA to easily evaluate the number of cells.

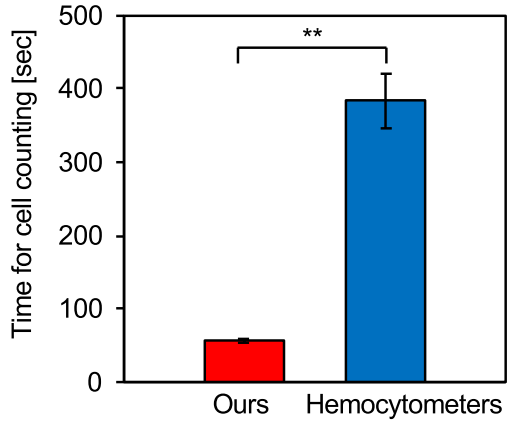

FIGURE 8. Comparison of the times required for analyses with our method and with the hemocytometer. Data are presented as mean ± standard deviation unpaired t-test, ** $p < 0.01$, $n = 3$.

hemocytometer (both of which are considered environmentally unsustainable) are required in the conventional method, but not in the proposed method [35]. Furthermore, the method is more readily applicable because the jig is the only special device required to apply the proposed method for practical use given the ubiquity of smartphones.

While we found that the accuracy and stability of the proposed method were statistically better compared with the conventional method, the actual cell number cannot be measured precisely. In this study, we defined the number of cells measured by an automatic cell counter as the true value, but there is no practical method to measure the exact cell number. In fact, even though there is a generalized protocol for bioengineering experiments, researchers need to make their own protocols. However, the exact number of cells is generally not of great importance. The estimated cell number derived with conventional methods is unreliable because of the numerous manual steps that are required to measure the cell number, as well as variation resulting from differences in the approach of individual technicians. Thus, the method proposed here is valuable in that it can serve as a consistent standard that is independent of technicians' skills.

Although our method provided superior accuracy and stability, further improvements could be achieved with two modifications (aside from simply increasing the size of the training datasets). The first involves the hardware, namely, modifying the size of the jig to obtain a clearer image with more consistent imaging conditions. Because of the gap between the jig, the tube, and the smartphone, the ROI can be shift within the image frame (Supplementary Fig. 1), and the focus of the image can shift (Supplementary Fig. 2); the latter of these issues is more problematic. This could be solved by the use of a larger jig with appropriate dimensions. This modification should yield images better suited to the training dataset, which would thus presumably improve the results of the proposed method. The CNN model predictions in this study were based on images captured from only two directions. However, cell aggregation occurs in three dimensions. Accordingly, the accuracy of the results could be further improved by modifying the jig to allow images to be captured from more directions. With regard to software improvements, the accuracy of the proposed method could be improved by changing the structure of the CNN model. The CNN model used in this study was based on a conventional architecture, VGG16 [36]. Future versions of the CNN model can be supplemented with modules, such as residual modules and attention modules, which have been reported to be effective in improving prediction accuracy [37], [38].

Here, we validated our method with a single cell type, constant centrifugation conditions, and one type of tube. Because cells of different species have different sizes, different centrifuging conditions result in cell aggregates of different sizes, even with a constant cell number [39], [40]. The jig used in this study was developed for a 15-mL tube, and cannot be used with other tube sizes. Thus, while we successfully demonstrated the potential performance of the proposed method, the results are specific to the conditions tested here. For our method to be used with other cell species, datasets must be collected for each cell species, and the CNN model must be trained by these datasets on the server to prepare a tailor-made trained model. These updates would make the present method more robust against conditions such as different cell species and various imaging conditions.

While several cutting-edge cell counting technologies have been proposed, there remains a need for techniques that do not require manual sampling and that can return results quickly for daily cell culture processes. In this study, we demonstrated the value of our novel cell counting method. We believe that our method has tremendous potential for easy cell number measurement in routine applications. To increase the ubiquity of the developed approach using macro-scale images, the CNN model can be incorporated into an automatic cell culture process rather than implementing a web application. The smartphone camera and jig could be replaced with higher quality equipment to improve and stabilize the imaging conditions, and thus facilitate the use of a CNN model with an automatic cell culture system.

V. CONCLUSION

In this paper, we introduced a novel cell counting method for estimating the cell number from images of a tube in which cells have been aggregated by centrifugation. The proposed method exhibited superior accuracy, stability, and convenience compared with the conventional and widely-used hemocytometer-based cell counting method. Our method is expected to be broadly applicable in bioengineering studies, and its implementation is expected to significantly reduce the burden of cell culture processes.

ACKNOWLEDGMENT

(Chikahiro Imashiro and Yuta Tokuoka contributed equally to this work.) The authors would like to thank for Dr. Shuichi Kurabayashi of Cygames, Inc., for his valuable advice in

the development of our idea. Chikahiro Imashiro and Yuta Tokuoka are JSPS Research Fellows.

REFERENCES

[1] R. Langer and J. Vacanti, "Tissue engineering," *Science*, vol. 260, no. 5110, pp. 920–926, May 1993.
[2] H. Lee, D. S. Kim, S. K. Ha, I. Choi, J. M. Lee, and J. H. Sung, "A pumpless multi-organ-on-a-chip (MOC) combined with a pharmacokinetic-pharmacodynamic (PK-PD) model," *Biotechnol. Bioeng.*, vol. 114, no. 2, pp. 432–443, Feb. 2017.
[3] J. Galle, M. Loeffler, and D. Drasdo, "Modeling the effect of deregulated proliferation and apoptosis on the growth dynamics of epithelial cell populations *in vitro*," *Biophysical J.*, vol. 88, no. 1, pp. 62–75, Jan. 2005.
[4] T. Yasaka, S. Ichisaka, T. Katsumoto, H. Maki, M. Saji, G. Kimura, and K. Ohno, "Apoptosis involved in density-dependent regulation of rat fibroblastic 3Y1 cell Culture.," *Cell Struct. Function*, vol. 21, no. 6, pp. 483–489, 1996.
[5] D. S. Kim, M. W. Lee, Y. J. Ko, Y. H. Chun, H. J. Kim, K. W. Sung, H. H. Koo, and K. H. Yoo, "Cell culture density affects the proliferation activity of human adipose tissue stem cells," *Cell Biochemistry Function*, vol. 34, no. 1, pp. 16–24, Jan. 2016.
[6] H. Tauchi, C. Imashiro, T. Kuribara, G. Fujii, Y. Kurashina, K. Totani, and K. Takemura, "Effective and intact cell detachment from a clinically ubiquitous culture flask by combining ultrasonic wave exposure and diluted trypsin," *Biotechnol. Bioprocess Eng.*, vol. 24, no. 3, pp. 536–543, Jul. 2019.
[7] C. Imashiro, Y. Kurashina, T. Kuribara, M. Hirano, K. Totani, and K. Takemura, "Cell patterning method on a clinically ubiquitous culture dish using acoustic pressure generated from resonance vibration of a disk-shaped ultrasonic transducer," *IEEE Trans. Biomed. Eng.*, vol. 66, no. 1, pp. 111–118, Jan. 2019.
[8] M. N. De Silva, J. Paulsen, M. J. Renn, and D. J. Odde, "Two-step cell patterning on planar and complex curved surfaces by precision spraying of polymers," *Biotechnol. Bioeng.*, vol. 93, no. 5, pp. 919–927, Apr. 2006.
[9] Y. Kurashina, C. Imashiro, M. Hirano, T. Kuribara, K. Totani, K. Ohnuma, J. Friend, and K. Takemura, "Enzyme-free release of adhered cells from standard culture dishes using intermittent ultrasonic traveling waves," *Commun. Biol.*, vol. 2, no. 1, pp. 1–11, Dec. 2019.
[10] M. Yang, N. Yang, S. Bi, X. He, L. Chen, Z. Zhu, Y. Gao, and Z. Du, "Micropatterned designs of thermoresponsive surfaces for modulating cell behaviors," *Polym. Adv. Technol.*, vol. 24, no. 12, pp. 1102–1109, Dec. 2013.
[11] T. Kakegawa, N. Mochizuki, N. Sadr, H. Suzuki, and J. Fukuda, "Cell-adhesive and cell-repulsive zwitterionic oligopeptides for micropatterning and rapid electrochemical detachment of cells," *Tissue Eng. A*, vol. 19, nos. 1–2, pp. 290–298, Jan. 2013.
[12] M. Nakao, Y. Kurashina, C. Imashiro, and K. Takemura, "A method for collecting single cell suspensions using an ultrasonic pump," *IEEE Trans. Biomed. Eng.*, vol. 65, no. 1, pp. 224–231, Jan. 2018.
[13] A. Mölder, M. Sebesta, M. Gustafsson, L. Gisselson, A. G. Wingren, and K. Alm, "Non-invasive, label-free cell counting and quantitative analysis of adherent cells using digital holography," *J. Microsc.*, vol. 232, no. 2, pp. 240–247, Oct. 2008.
[14] H. Lu, O. Caen, J. Vrignon, E. Zonta, Z. El Harrak, P. Nizard, J.-C. Baret, and V. Taly, "High throughput single cell counting in droplet-based microfluidics," *Sci. Rep.*, vol. 7, no. 1, pp. 1–9, Dec. 2017.
[15] S. Chakraborty, C. Das, K. Ghoshal, M. Bhattacharyya, A. Karmakar, and S. Chattopadhyay, "Low frequency impedimetric cell counting: Analytical modeling and measurements," *IRBM*, vol. 41, no. 1, pp. 23–30, Feb. 2020.
[16] A. Aijaz, D. Trawinski, S. McKirgan, and B. Parekkadan, "Non-invasive cell counting of adherent, suspended and encapsulated mammalian cells using optical density," *BioTechniques*, vol. 68, no. 1, pp. 35–40, Jan. 2020.
[17] T. Takahashi, "Applicability of automated cell counter with a chlorophyll detector in routine management of microalgae," *Sci. Rep.*, vol. 8, no. 1, pp. 1–12, Dec. 2018.
[18] T. Falk, D. Mai, R. Bensch, Ö. Çicek, A. Abdulkadir, Y. Marrakchi, A. Böhm, J. Deubner, Z. Jäckel, K. Seiwald, and A. Dovzhenko, "U-net: Deep learning for cell counting, detection, and morphometry," *Nature Methods*, vol. 16, no. 1, pp. 67–70, Jan. 2019.
[19] Y. Fukuma, T. Inui, C. Imashiro, Y. Kurashina, and K. Takemura, "Homogenization of initial cell distribution by secondary flow of medium improves cell culture efficiency," *PLoS ONE*, vol. 15, no. 7, Jul. 2020, Art. no. e0235827.
[20] N. Yachie *et al.*, "Robotic crowd biology with Maholo LabDroids," *Nature Biotechnol.*, vol. 35, pp. 310–312, Apr. 2017, doi: 10.1038/nbt.3758.
[21] M. Ooka, Y. Tokuoka, S. Nishimoto, N. F. Hiroi, T. G. Yamada, and A. Funahashi, "Deep learning for non-invasive determination of the differentiation status of human neuronal cells by using phase-contrast photomicrographs," *Appl. Sci.*, vol. 9, no. 24, p. 5503, Dec. 2019.
[22] D. Silver, J. Schrittwieser, K. Simonyan, I. Antonoglou, A. Huang, A. Guez, T. Hubert, L. Baker, M. Lai, A. Bolton, Y. Chen, T. Lillicrap, F. Hui, L. Sifre, G. van den Driessche, T. Graepel, and D. Hassabis, "Mastering the game of go without human knowledge," *Nature*, vol. 550, no. 7676, pp. 354–359, Oct. 2017.
[23] S. Nishimoto, Y. Tokuoka, T. G. Yamada, N. F. Hiroi, and A. Funahashi, "Predicting the future direction of cell movement with convolutional neural networks," *PLoS ONE*, vol. 14, no. 9, Sep. 2019, Art. no. e0221245.
[24] O. Ronneberger, P. Fischer, and T. Brox, "U-net: Convolutional networks for biomedical image segmentation," in *Medical Image Computing and Computer-Assisted Intervention* (Lecture Notes in Computer Science: Lecture Notes in Artificial Intelligence and Lecture Notes in Bioinformatics), vol. 9351. Cham, Switzerland: Springer, 2015, pp. 234–241.
[25] A. Krizhevsky, I. Sutskever, and G. E. Hinton, "ImageNet classification with deep convolutional neural networks," in *Proc. Adv. Neural Inf. Process. Syst. (NIPS)*, vol. 1, 2012, pp. 1097–1105.
[26] D. Zhang and Q. Liu, "Biosensors and bioelectronics on smartphone for portable biochemical detection," *Biosensors Bioelectron.*, vol. 75, pp. 273–284, Jan. 2016.
[27] G. L. Damhorst, C. Duarte-Guevara, W. Chen, T. Ghonge, B. T. Cunningham, and R. Bashir, "Smartphone-imaged HIV-1 reverse-transcription loop-mediated isothermal amplification (RT-LAMP) on a chip from whole blood," *Engineering*, vol. 1, no. 3, pp. 324–335, Sep. 2015.
[28] S. Choi, "Powering point-of-care diagnostic devices," *Biotechnol. Adv.*, vol. 34, no. 3, pp. 321–330, May 2016.
[29] G. P. Zhang, "Avoiding pitfalls in neural network research," *IEEE Trans. Syst., Man Cybern. C, Appl. Rev.*, vol. 37, no. 1, pp. 3–16, Jan. 2007.
[30] V. Nair and G. E. Hinton, "Rectified linear units improve restricted Boltzmann machines," in *Proc. 27th Int. Conf. Mach. Learn. (ICML)*, 2010, pp. 807–814.
[31] N. Srivastava, G. Hinton, A. Krizhevsky, I. Sutskever, and R. Salakhutdinov, "Dropout: A simple way to prevent neural networks from overfitting," *J. Mach. Learn. Res.*, vol. 15, no. 1, pp. 1929–1958, 2014.
[32] S. Tokui, K. Oono, S. Hido, and J. Clayton, "Chainer: A next-generation open source framework for deep learning," in *Proc. 29th Workshop Mach. Learn. Syst. Neural Inf. Process. Syst. (NIPS)*, vol. 5, Dec. 2015, pp. 1–6.
[33] Z. Gao, L. Wang, L. Zhou, and J. Zhang, "HEp-2 cell image classification with deep convolutional neural networks," *IEEE J. Biomed. Health Informat.*, vol. 21, no. 2, pp. 416–428, Mar. 2017.
[34] I. Lawrence and K. Lin, "A concordance correlation coefficient to evaluate reproducibility," *Biometrics*, vol. 45, no. 1, pp. 255–268, Mar. 1989.
[35] S. Kothari and W. Harcourt, "Introduction: The violence of development," *Development*, vol. 47, no. 1, pp. 3–7, Mar. 2004.
[36] K. Simonyan and A. Zisserman, "Very deep convolutional networks for large-scale image recognition," in *Proc. 3rd Int. Conf. Learn. Representations (ICLR)*, 2015. [Online]. Available: https://arxiv.org/abs/1409.1556
[37] K. He, X. Zhang, S. Ren, and J. Sun, "Deep residual learning for image recognition," in *Proc. IEEE Conf. Comput. Vis. Pattern Recognit. (CVPR)*, Jun. 2016, pp. 770–778.
[38] F. Wang, M. Jiang, C. Qian, S. Yang, C. Li, H. Zhang, X. Wang, and X. Tang, "Residual attention network for image classification," in *Proc. IEEE Conf. Comput. Vis. Pattern Recognit. (CVPR)*, Jul. 2017, pp. 6450–6458.
[39] N. Senda and K. Osawa, "Cell sheets image validation of phase-diversity homodyne OCT and effect of the light irradiation on cells," *Imag., Manipulation, Anal. Biomolecules, Cells, Tissues IX*, vol. 9711, Apr. 2016, Art. no. 97110F.

[40] E. K. Eskov, "Development of socialty in the bee superfamily (Hymenoptera, Apoidea)," *J. Evol. Biochemistry Physiol.*, vol. 50, no. 5, pp. 363–382, Sep. 2014.

CHIKAHIRO IMASHIRO received the B.E. degree in mechanical engineering and the M.E. and Ph.D. degrees from the School of Science and Technology, Keio University, Yokohama, Japan, in 2015, 2017, and 2019, respectively. He was a Research Assistant with the Leading Graduate Schools program, Japan, from 2015 to 2018, and a Research Fellow with the Japan Society of the Promotion of Science (DC2) from 2018 to 2019. He is currently a Research Fellow with the Japan Society of the Promotion of Science (PD), Tokyo Women's Medical University. His research interests include ultrasonic transducers, tissue engineering, biomedical devices, and mechanobiology.

YUTA TOKUOKA received the B.E. and M.E. degrees in biosciences and informatics from Keio University, in 2016 and 2018, respectively, where he is currently pursuing the Ph.D. degree under the supervision of Dr. A. Funahashi. He joined the School of Fundamental Science and Technology, Keio University, in 2018. He is currently a Research Fellow (DC2) with the Japan Society for the Promotion of Science. His research interests include computer vision, machine learning, and developmental biology.

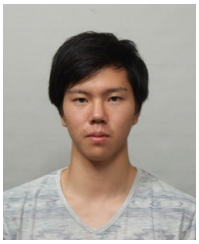

KAITO KIKUHARA received the B.A. degree in environment and information studies and the M.M.G. degree in media and governance from Keio University, Japan, in 2018 and 2020, respectively, where he is currently pursuing the Ph.D. degree under the supervision of Dr. K. Takemura. He joined the School of Fundamental Science and Technology, Keio University, in 2020. He was a Research Assistant with the Leading Graduate Schools program, Japan, from 2018 to 2020. His research interests include haptics, semantic computing, and mathematical model.

TAKAHIRO G. YAMADA received the B.S. and M.S. degrees in biosciences and informatics from Keio University, in 2015 and 2017, respectively, where he is currently pursuing the Ph.D. degree under the supervision of Dr. A. Funahashi. He joined the School of Fundamental Science and Technology, Keio University, in 2017, where he has been a Research Associate with the Department of Biosciences and Informatics, since 2017. His research interests include systems biology, bioinformatics, and biophysics.

KENJIRO TAKEMURA (Member, IEEE) received the B.E. degree in mechanical engineering, the M.E. degree in biomedical engineering, and the Ph.D. degree in integrated design engineering from Keio University, Yokohama, Japan, in 1998, 2000, and 2002, respectively. He was a Research Associate with the Department of Mechanical Engineering, Keio University, in 2002, and an Assistant Professor with the Precision and Intelligence Laboratory, Tokyo Institute of Technology, from 2003 to 2008. He has been with the Department of Mechanical Engineering, Keio University, since 2008, where he is currently a Professor. His research interests are on ultrasonic transducers, functional fluids, haptic interface, and biomedical devices.

AKIRA FUNAHASHI received the B.E. degree in electrical engineering and the M.E. and Ph.D. degrees in computer science from Keio University, Japan, in 1995, 1997, and 2000, respectively. He was a Research Fellow with the Japan Society of the Promotion of Science (DC1) from 1997 to 2000 and a Research Associate with the Department of Information Technology, Mie University, Japan, from 2000 to 2002. In 2007, he then joined the Kitano Symbiotic Systems Project, JST, and The Systems Biology Institute, as a Researcher. He is currently an Associate Professor with the Department of Biosciences and Informatics, Keio University. His research interests include systems biology, quantitative biology, parallel processing, and machine learning.